ELSEVIER

Journal of Photochemistry and Photobiology A: Chemistry 101 (1996) 205–214

Journal of PHOTOCHEMISTRY AND PHOTOBIOLOGY A:CHEMISTRY

Photochemistry of azobenzenophanes with three-membered bridges

Dirk Röttger, Hermann Rau *

FG Physikalische Chemie, Institut für Chemie, Universität Hohenheim, D-70593 Stuttgart, Germany

Received 2 January 1996; accepted 28 March 1996

Abstract

Azobenzenophanes may be suitable precursor molecules for tetrazetidines with a four-membered nitrogen ring. The synthesis and photochemistry of azobenzenophanes with at least one three-carbon bridge are reported. The photochemistry is dominated by $E \Leftrightarrow Z$ isomerization. This class of azobenzenophanes has thermally stable Z,Z isomers, probably due to the rigidity of the three-carbon bridge. This stiffness, however, hampers tetrazetidine formation. Some clues to tetrazetidine formation are presented and an unusual thermal isomerization $E,E \rightarrow E,Z$ is reported.

Keywords: Azobenzene; Mauser diagrams; Phane; Photoisomerization; Tetrazetidine

1. Introduction

Azobenzenophanes **1**, **2** and **3** and phane **4** may be suitable precursor molecules for tetrazetidines (tetraazacyclobutanes), a class of simple cyclic molecules with a four-membered nitrogen ring not yet prepared. Only indirect evidence of these compounds exists, e.g. from a photometathesis of a tailormade aliphatic azoxy/azo compound [1] and kinetic analysis of the photoreaction [2] of an azobenzenophane. In the azobenzenophanes, the four-nitrogen ring structure is preformed, and photochemical ring formation may have a chance against predominant geometrical *E–Z* isomerization. Recently, we have reported sound theoretical arguments for the kinetic stability of the tetrazetidine system and for the formation of tetrazetidine on high-energy $\pi \rightarrow \pi^*$ excitation of the azobenzene unit, but not on $n \rightarrow \pi^*$ excitation [2]. In Ref. [2], we also published indirect experimental evidence for the formation of tetrazetidine from **1**, but as an isolated material tetrazetidine is still evasive.

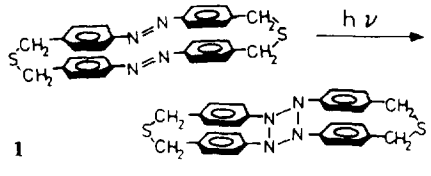

1

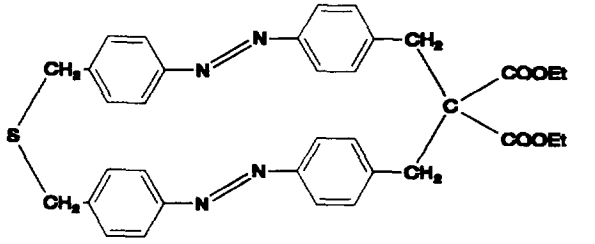

2

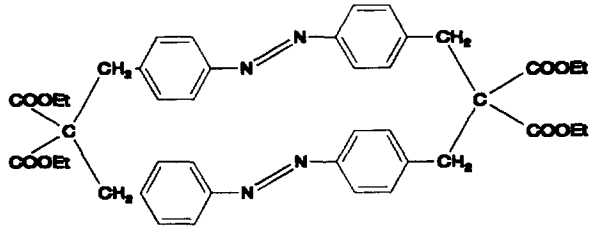

3

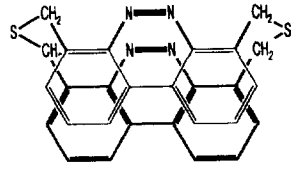

4

The azobenzenophanes with $-CH_2-S-CH_2-$ bridges, such as **1**, are hardly soluble; **4** is virtually insoluble [3]. As the kinetic species, which we have attributed to tetrazetidine [2], is short lived, we assume fast ring opening which should be thermally activated. Thus low-temperature experiments are necessary, and this requires better solubility which can be obtained by substitution of the phanes. Substitution in the

* Corresponding author.

PII S1010-6030(96)04355-9

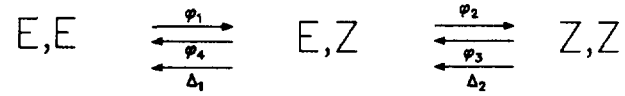

Scheme 1.

ortho positions in the azobenzene rings will hinder the approach of the azo groups during the course of tetrazetidine formation; substitutions in the meta positions may give problems when para bridges are synthesized; therefore we chose the bridge for the substitutions and synthesized **2** and **3**. This approach was successful, and no limitations for photokinetic experiments on solubility grounds remained.

The results of irradiation experiments on azobenzenophanes showed that consecutive *Z–E* isomerizations (Scheme 1) are the main photo and thermal reactions; this is not unexpected [3]. From a kinetic analysis, we extracted all four quantum yields of the main reactions [4]. The three-carbon bridges seem to increase the rigidity of the framework of the structure, rather than the sulphur-containing bridges. An unusual long-term stability of the *Z,Z* form of **2** and **3** was found, in addition to a surprising side reaction which is characterized by thermal *E* to *Z* isomerization. Hints to tetrazetidine formation are weaker than for **1**. A certain degree of flexibility seems to be necessary to accommodate the changes in the distance of the azo groups on ring formation in the azobenzenophanes.

2. Experimental details

2.1. Synthesis of azobenzenophanes 2 and 3 [4]

The critical step in the synthesis of **2** and **3** is the closure of the cyclophane ring. The syntheses seem to be straightforward, but this impression is deceptive [4].

The synthesis can be attempted by reducing the nitro groups to form azo groups. This route (employing $LiAlH_4$) was used successfully by Tamaoki et al. [5], even for the azobenzenophane with $-CH_2-CH_2-$ bridges, but starting from 2,2-di-EtOOC-1,3-bis(*p*-nitrophenyl)propane **5** we could not isolate the target molecule **3** from the reaction mixture. Electroreduction of **5** provided the doubly reduced **3** in very small amounts and the monoazo compound **6** in larger amounts. Therefore we synthesized **6** as shown in Scheme 2 by coupling two malonic ester units with one bis-bromomethyl-azobenzene and subsequent substitution of the remaining H atom at the malonic acid central C atom by *p*-nitrobenzyl units. Then **6** was subjected to electroreduction to give a few milligrams of **3**.

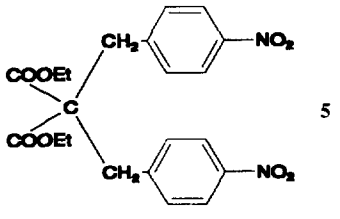

5

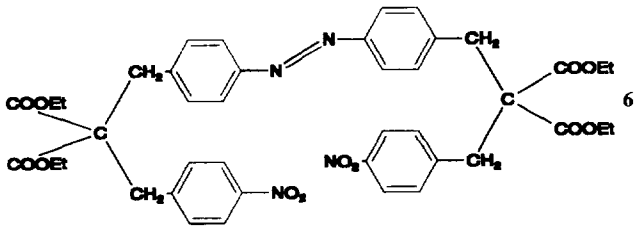

6

For **2**, the best method involves the preparation of $(EtCOO)_2C(CH_2–Ph–N=N–Ph–CH_2–Br)_2$ by alkylation of one molecule of malonic ester and two molecules of 4-bromomethyl-4′-methylazobenzene, and subsequent bromination of the methyl group. With Na_2S, the cyclophane ring can be closed (Scheme 3). The yields were not optimized, but were in the region of about 5% on the basis of the amount of dimethylazobenzene. Other attempts were not sufficiently successful [4].

Compound **4** was prepared in a four-step synthesis by photocyclization of *o,o′*-dimethylazobenzene in acid solution, bromination of the dimethylbenzo[c]cinnoline, substitution of the bromo by –SH groups and coupling of the bis-bromomethyl and bis-methylthiolbenzo[c]cinnolines. It is not sufficiently soluble for cyclization experiments.

2.2. Irradiation and analysis set-up

For irradiation and photokinetic experiments, a new apparatus was used (Fig. 1) which integrates both functions of irradiation and analysis [4]. The key feature is the collinearity of the irradiation and analysis beams. This geometry was selected since, in viscous or solid solutions, one of the requirements for photokinetic evaluation, the homogeneous distribution of all molecular species, is no longer guaranteed. Under these conditions, the experiments can still be analysed when a collinear geometry is used, but not when a right angle geometry is employed.

The set-up consists of a single-beam spectrophotometer with a deuterium lamp (Zeiss CLD 300) and a diode array detector (Zeiss MCS 220) with 512 diodes, each 2 nm in width. The spectro-beam is guided by waveguides and made parallel before it travels through the sample cell. The sample is placed in a home-built housing whose temperature can be

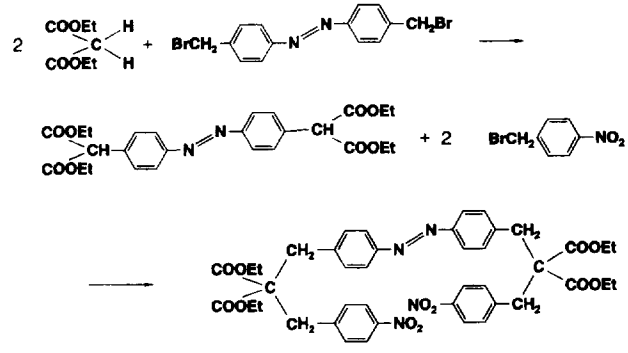

Scheme 2.

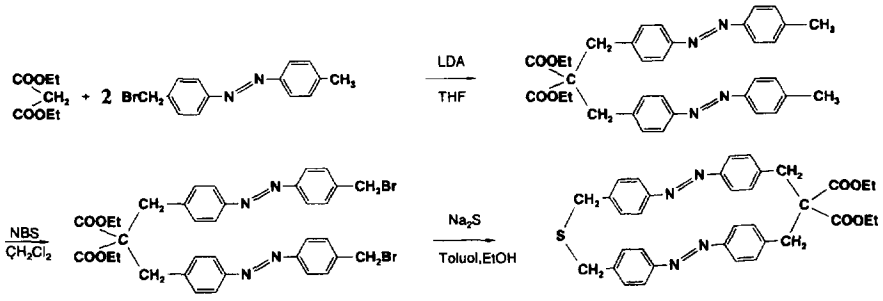

Scheme 3.

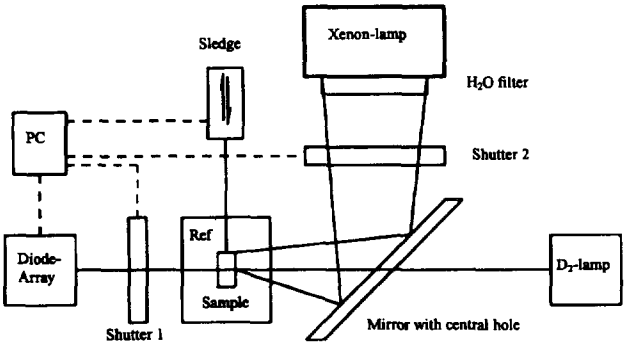

Fig. 1. Experimental set-up (for explanation, see text).

adjusted by a liquid thermostat and whose windows can be purged by a stream of dry gas in order to avoid fogging. The sample cell can be replaced at any time by a reference cell in order to record a new baseline. The photolysing radiation from a water-cooled 150 W xenon source (PTI) has a large diameter; under suitable focusing, it passes an interference filter and is deflected by a mirror onto the sample cell. The mirror has a central bore for the spectro-beam which is much narrower than the area covered by the irradiation beam from the xenon lamp. Two shutters are used to switch from the irradiation to the analysing mode and back. They protect the diode array from the high-intensity radiation of the xenon lamp. An additional shutter closes the deuterium lamp path during monochromatic irradiation by the xenon source. The experiments are computer controlled by means of the program MESSEN 3.5 [6]. The irradiation periods can be selected down to 1 s; the minimum reading period is 40 ms. Therefore quite rapid reactions can be resolved.

The program MESSEN 3.5 acquires the spectral data. Pascal programs were written for evaluation; the data are converted to a format suited for the SIGMAPLOT® package.

3. Results

3.1. Photoreactions of the azobenzenophane 2

Fig. 2 shows the room temperature reaction spectra of **2** in acetonitrile on irradiation at 366 nm. On inspection, blurred isosbestic points can be seen which indicate more than one

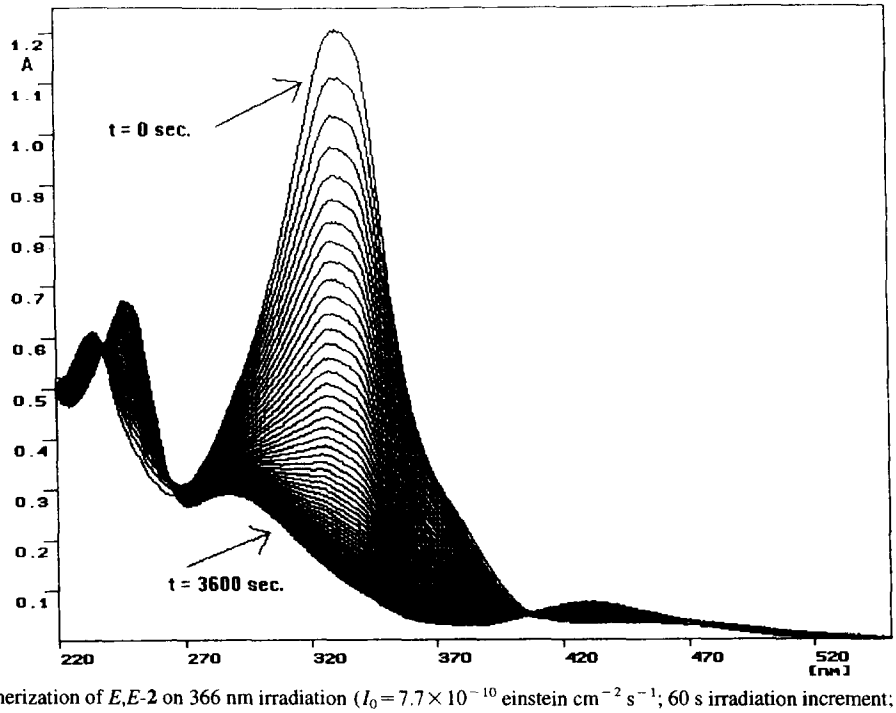

Fig. 2. Photoisomerization of *E,E*-**2** on 366 nm irradiation ($I_0 = 7.7 \times 10^{-10}$ einstein cm^{-2} s^{-1}; 60 s irradiation increment; $c = 2.5 \times 10^{-5}$ M).

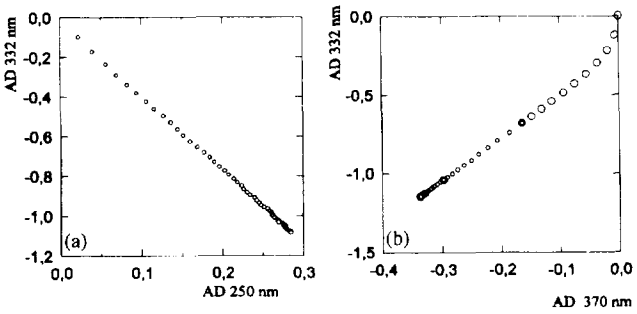

Fig. 3. AD-diagrams of the photoreaction of *E,E*-**2** induced by 366 nm irradiation: (a) wavelengths 332 and 250 nm; (b) wavelengths 332 and 370 nm.

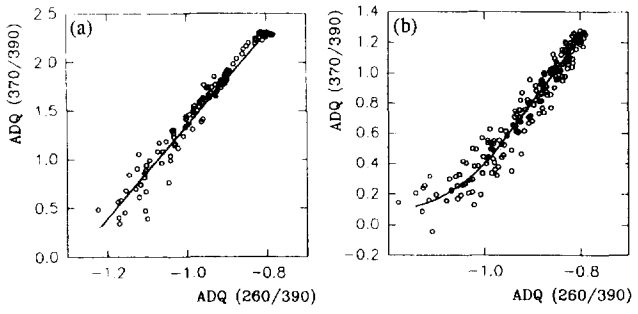

Fig. 4. ADQ diagrams of the photoreaction of *E,E*-**2** induced by 366 nm irradiation: (a) at room temperature; (b) at 353 K.

reaction step. The graphical matrix rank analysis [7] of this photoreaction (Mauser diagrams [1]) gives linear and non-linear AD diagrams, depending on the wavelengths selected for the diagrams (Fig. 3). This is used later for the determination of the quantum yields (see Section 3.3).

On irradiation at 366 nm, most of the Mauser ADQ plots constructed from the data of Fig. 2 are linear (Fig. 4); some may be non-linear indicating an additional independent reaction. At 243 K, the non-linearity is more obvious, but still small. On irradiation at 436 nm, however, the ADQ diagrams are linear at room and at low temperature.

As the non-linearity of the ADQ plots is not very obvious by graphical matrix rank analysis, a numerical procedure was employed [8,9]. A matrix ΔA of the absorbance differences $\Delta A_{i,j}$ was created with the wavelength dependence in the rows and the time dependence in the columns. After proper transformation of the matrix, the rank is given by the number of non-zero diagonal elements. However, these elements are not integers and thus we need a threshold criterion. This is given by the requirement that the error is smaller than the diagonal element. The errors $S_{i,j}$ for all experimental $\Delta A_{i,j}$ values are independent of each other. We estimated that there is little variation in the errors for different wavelengths and for different values of the absorbance, and thus used the equipment-determined error of 0.004 absorption units for all matrix elements $S_{i,j}$. From this numerical matrix rank analysis, we obtain $s=2$ for irradiation at room temperature, irrespective of the irradiation wavelength. However, at 243 K, we find that $s=3$ for $\pi \rightarrow \pi^*$ irradiation (366 nm) and $s=2$ for $n \rightarrow \pi^*$ irradiation (436 nm), which is in agreement with the graphical analysis.

Long-term irradiation at 313 nm, which leads to excitation of the π,π^* state of **2**, but is also absorbed by the possible formation of tetrazetidine [2], leads to total disintegration of molecule **2** by primary and secondary photoreactions. There are at least 30 different products after 3 days of 313 nm irradiation. At least five are orange and non-fluorescent on a chromatographic thin layer (obviously azobenzene derivatives). Many of the other spots are fluorescent. In contrast, in a parallel experiment with long-term irradiation of **2** at 366 nm, only the *Z,Z* and *E,E* isomers are detected; the molecule is not destroyed. Moreover, the two non-cyclophane compounds $S(CH_2\text{–}Ph\text{–}N{=}N\text{–}Ph\text{–}CH_3)_2$ and $(C_2H_5OOC)_2C\text{-}(CH_2\text{–}Ph\text{–}N{=}N\text{–}Ph\text{–}CH_3)_2$, derived from **2** by cutting out the malonic ester unit or the sulphur atom, do not decompose on 313 nm irradiation.

Irradiation of *E,E*-**2** at 366 nm in a solid matrix of 96% EtOH at 77 K does not lead to the same photostationary state as that obtained at room temperature; $E \rightarrow Z$ isomerization is inhibited. On the other hand, when a solution in the photostationary state after 366 nm irradiation at room temperature, which consists of more than 90% of the *Z,Z* isomer, is frozen to 77 K and irradiated in a rigid solvent by 436 nm light, the system is totally converted to the *E,E* isomer, far beyond the photostationary state at room temperature. This parallels azobenzene behaviour, where $E \rightarrow Z$ isomerization is negligible, but $Z \rightarrow E$ isomerization is still possible in rigid solvents at low temperature.

3.2. Thermal reactions of the azobenzenophane 2

It is well known that the *Z* isomers of azobenzene and its derivatives are thermally unstable. In the azobenzenophane **1**, pre-irradiated at 366 nm, we observed [2,3] a fast ($k_{298}=1.6\times10^{-6}$ s^{-1}, $E_a=96.2$ kJ mol^{-1}, toluene) and slow ($k_{298}=1.85\times10^{-3}$ s^{-1}, $E_a=82.9$ kJ mol^{-1}, toluene) thermal *Z–E* isomerization, which we attributed to the $Z,E \rightarrow E,E$ and $Z,Z \rightarrow Z,E$ reactions respectively. In the cyclophanes **2** and **3**, the photoisomerization leads to photostationary states rich in the *Z,Z* isomer if an appropriate wavelength is chosen. On shutting off the irradiation source, we again

[1] Mauser diagrams provide information about the number of linearly independent reactions in a reaction system. The values of the absorbance A_{λ_1} or the absorbance difference ΔA_{λ_1} (usually the change relative to the starting value) at one arbitrary wavelength λ_1, taken from a series of reaction spectra (as in Fig. 2), are plotted vs. the corresponding values A_{λ_2} or ΔA_{λ_2} at a different wavelength λ_2 (A diagrams or AD diagrams). If a straight line results, there is only one independent reaction ($s=1$); if the plot is non-linear, there is more than one reaction ($s>1$). In this case, the absorbance differences at the two arbitrary wavelengths are referred to the absorbance difference at a third wavelength (absorbance difference quotient), and ADQ plots of $\Delta A_{\lambda_1}/\Delta A_{\lambda_3}$ vs. $\Delta A_{\lambda_2}/\Delta A_{\lambda_3}$ are created. If they are linear, there are only two independent reactions in the system ($s=2$); if they are non-linear, there are more than two ($s>2$). Higher order diagrams can be constructed in principle, but they can only be evaluated when the error margin of the experimental data is very low, as the ratio of differences has an unfavourable progression of errors.

observe a fast (Δ_1) and a very slow (Δ_2) thermal reaction. Δ_1 can be assigned to the $Z,E \rightarrow E,E$ reaction and Δ_2 to the $Z,Z \rightarrow Z,E$ reaction. The very slow reaction Δ_2 can be evaluated according to first-order kinetics when one point per week is recorded, and the pure E,E isomer is assumed to be the final product. By using the "formal integration" method of Mauser [7]

$$\frac{\Delta A_\lambda}{t'-t} = kA_{\lambda\infty} - k\frac{\int_t^{t'} A_\lambda \mathrm{d}t}{t'-t} \quad (1)$$

we do not need to know $A_{\lambda\infty}$, the absorbance at infinite time, to determine k. We arrive at a lifetime of the Z,Z isomer of more than 1 year (this lifetime may be even longer, because during the course of the thermal isomerization experiments we cannot be totally sure that absolutely no light impinges on the sample). The reaction of **2** is at least 80 times slower than that of **1** and 200 times slower than that of 4,4′-dimethylazobenzene. The Z,Z isomer of **2** is virtually thermally stable. This allows the isolation of Z,Z-**2**. The fast reaction Δ_1 has a first-order rate constant of about $k_{298} = 8 \times 10^{-4}\ \mathrm{s}^{-1}$ ($E_a = 92\ \mathrm{kJ\ mol}^{-1}$) in acetonitrile, and this is independent of whether the thermal reaction is monitored after 366 nm irradiation of the E,E isomer or 436 nm irradiation of the Z,Z isomer.

Careful analysis of the thermal reactions reveals two additional very rapid reactions Δ_3 and Δ_4, which are only observed in a limited temperature interval of about 293–258 K. In order to detect them, the irradiation must not be interrupted to take the reaction spectra, because as much E,Z-**2** as possible must be accumulated.

After 10 min of continuous 366 nm irradiation (the photostationary state has not yet been reached), with an overall shift of E to Z configuration, the Δ_3 reaction precedes the Δ_1 reaction. Fig. 5(a) shows the absorption in the initial stage of the thermal reaction after shutting off the 366 nm light. The Δ_3 reaction seems to be too fast at 313 K and too slow at 253 K to be detected, which indicates a high energy of activation. The difference between the spectra taken at $t = 0$ s and $t = 400$ s is shown in Fig. 5(b), together with the spectra of E,E-**2** and Z,Z-**2**. It is obvious that Δ_3 involves $Z \rightarrow E$ isomerization, which is not surprising.

The same experiment starting from Z,Z-**2**, with 436 nm irradiation, is shown in Fig. 6(a). Again, the irradiation is not interrupted in order to produce a high concentration of the E,Z form, but is stopped before the photostationary state is reached. Here the photoreaction causes an increase in absorbance at the monitoring wavelength of 332 nm, representing overall $Z \rightarrow E$ isomerization. Again, after shutting off the 436 nm light, we observe a very fast reaction, Δ_4, which causes a decrease in absorbance. The difference spectrum of this experiment at $T = 273$ K is shown in Fig. 6(b); this indicates thermal $E \rightarrow Z$ isomerization, a reaction which, to our knowledge, has not been observed previously. Clearly, reactions Δ_3 and Δ_4 do not dominate the reaction system. However, they should not be overlooked. That they are not simple artefacts has been proven by a parallel experiment with azobenzene, in which no such fast reactions were observed.

3.3. Determination of the absorption coefficients of E,Z-2 and the quantum yields of the photoreactions of 2

Both E,E-**2** and Z,Z-**2** are stable compounds and their absorption coefficients can be determined in the usual way. For the particular isomerization system of compound **2**, the absorption coefficient of Z,E-**2** can be obtained as there are combinations of wavelengths whose AD diagrams are linear and others where this is not the case. Linearity in the AD diagrams in an $E,E \rightarrow E,Z \rightarrow Z,Z$ sequence is only possible if $\varepsilon_{E,Z} = 1/2(\varepsilon_{Z,Z} + \varepsilon_{E,E})$. This suggests non-interacting azobenzene units. However, there are also non-linear AD diagrams indicating interactions; the non-linearity is more expressed when one of the monitoring wavelengths is chosen in the "cyclophane" band around 380 nm.

For the determination of $\varepsilon_{E,Z}$, we evaluate the thermal reaction of **2** following irradiation [10]. Only the $E,Z \rightarrow E,E$ isomerization proceeds, as the Z,Z form is stable. Thus for $d = 1$ cm and a total concentration of c_0

$$A_{(t=0)} = \varepsilon_{Z,Z}c_{Z,Z(t=0)} + \varepsilon_{E,Z}c_{E,Z(t=0)} + \varepsilon_{E,E}c_{E,E(t=0)} \quad (2)$$

$$A_{(t=\infty)} = \varepsilon_{Z,Z}c_{Z,Z(t=0)} + \varepsilon_{E,E}c_{E,E(t=\infty)} = \varepsilon_{Z,Z}c_0 + (\varepsilon_{E,E} - \varepsilon_{Z,Z})c_{E,E(t=\infty)} \quad (3)$$

With $c_{E,Z(t=0)} = c_{E,E(t=\infty)} - c_{E,E(t=0)}$ and $\varepsilon_{E,Z} = 1/2(\varepsilon_{E,E} + \varepsilon_{Z,Z})$, we can derive

$$c_{E,E(t=0)} = \frac{A_{(t=0)} - [\varepsilon_{Z,Z}c_{Z,Z} - 1/2(\varepsilon_{E,E} + \varepsilon_{Z,Z})c_{E,E(t=\infty)}]}{\varepsilon_{E,E} - 1/2(\varepsilon_{E,E} + \varepsilon_{Z,Z})} \quad (4)$$

The other concentrations at the end of irradiation ($t = 0$) are: $c_{Z,Z(t=0)} = c_{Z,Z(t=\infty)} = c_{Z,Z} = [A_{(t=\infty)} - \varepsilon_{E,E}c_{E,E(t=\infty)}]/\varepsilon_{Z,Z}$ and $c_{E,Z(t=0)} = c_{E,E(t=\infty)} - c_{E,E(t=0)}$.

These concentrations at the end of irradiation are, of course, independent of the monitoring wavelength. Thus we can calculate the absorption coefficients of the E,Z form at wavelengths at which the AD diagram is not linear. To this end, the absorbance–time relation of the thermal reaction is fitted by variation of $\varepsilon_{E,Z}$ with

$$c_{E,Z(t)} = c_{E,Z(t=0)}\mathrm{e}^{-k_1 t} \quad (5)$$

$$c_{E,E(t)} = c_{E,E(t=0)} + (c_{E,Z(t=0)} - c_{E,Z(t)}) \quad (6)$$

$$A_t = \varepsilon_{Z,Z}c_{Z,Z} + \varepsilon_{E,Z}c_{E,Z(t)} + \varepsilon_{E,E}c_{E,E(t)} \quad (7)$$

using the values of k_1, $c_{E,E(t=0)}$, $c_{Z,Z}$, $\varepsilon_{E,E}$ and $\varepsilon_{Z,Z}$ determined before. Fitting was performed at 10 nm intervals. The results are shown in Fig. 7, together with the absorption spectra of E,E-**2** and Z,Z-**2**. The most important feature of the E,Z-**2** spectrum is the loss of the "cyclophane" band around 380

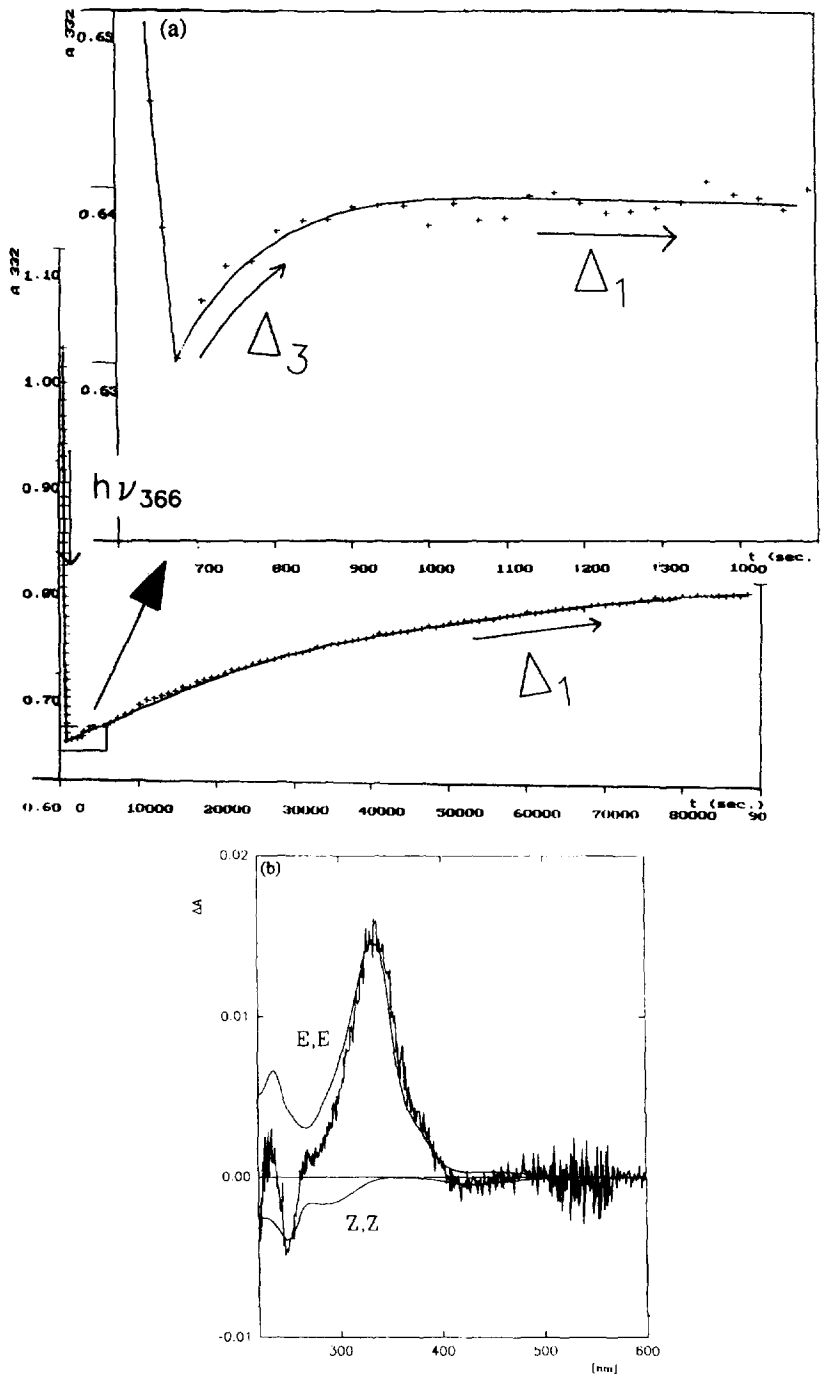

Fig. 5. (a) Absorbance changes during photoreaction induced by 366 nm irradiation (the very rapid thermal reaction Δ_3 and the thermal reaction Δ_1); (b) the difference spectrum due to Δ_3.

nm, which indicates the disappearance of the interactions between the cis and trans azobenzene moieties.

The determination of the photochemical quantum yields for the $E,E \rightarrow E,Z$ and $Z,Z \rightarrow E,Z$ reactions is possible from an evaluation of the initial slope of the reactions according to "formal integration" [11] by

$$\frac{\Delta A_\lambda}{\int F\mathrm{d}t} = \frac{1000 I_0 \varepsilon'_M \varphi_M A_{\lambda(\infty)} \int F\mathrm{d}t}{\int F\mathrm{d}t} - \frac{1000 I_0 \varepsilon'_M \varphi_M \int F A_\lambda \mathrm{d}t}{\int F\mathrm{d}t} \quad (8)$$

where F is the photokinetic factor $(1-10^{-A'})/A'$, λ is the analysis wavelength, the prime indicates the excitation wavelength and M is the absorbing molecule. The evaluation of the initial slope of the left-hand side vs. $\int F A_\lambda \mathrm{d}t$ provides the quantum yield. The results for azobenzenophane **2** are

$$\varphi_{E,E \rightarrow E,Z} = 0.23 \pm 0.03 \quad (9)$$

and

$$\varphi_{Z,Z \rightarrow E,Z} = 0.28 \pm 0.04 \quad (10)$$

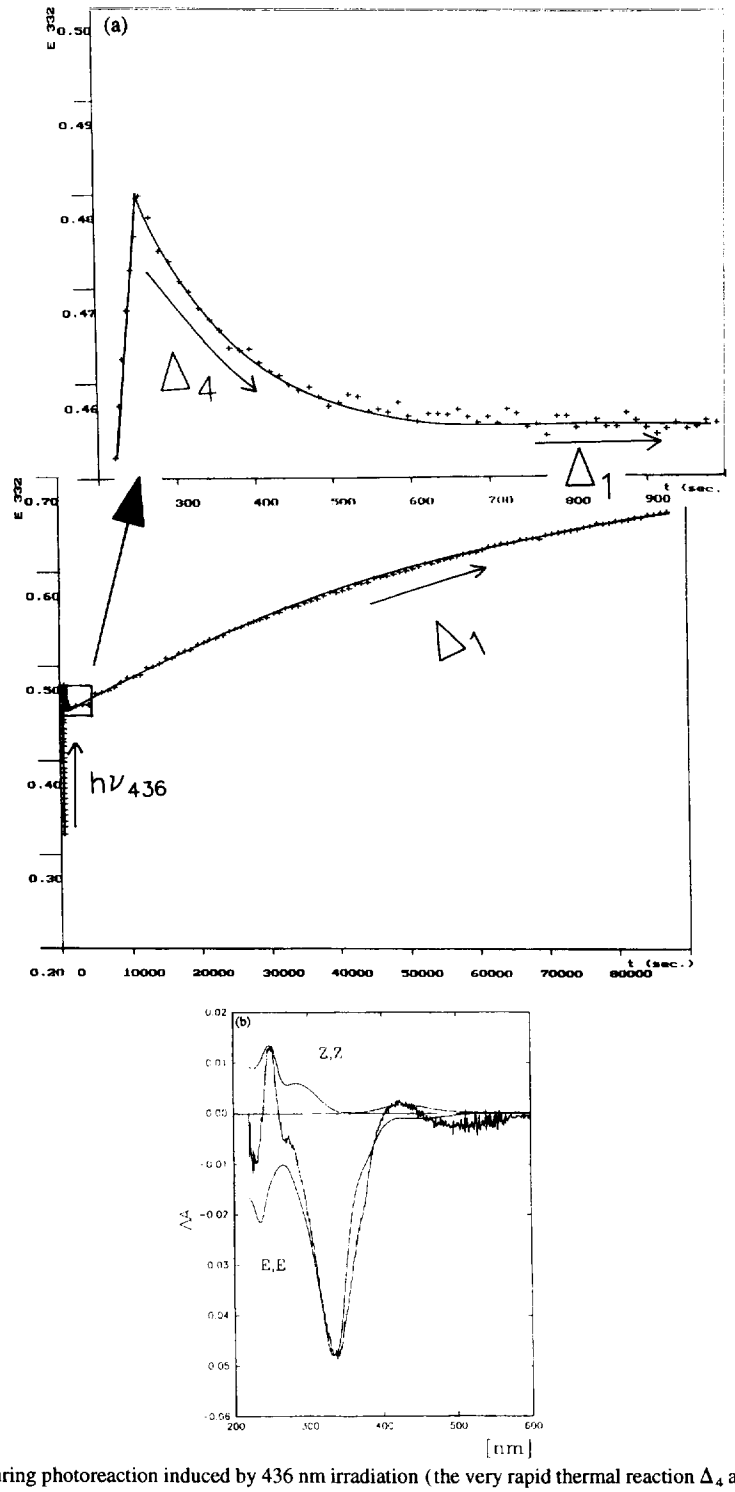

Fig. 6. (a) Absorbance changes during photoreaction induced by 436 nm irradiation (the very rapid thermal reaction Δ_4 and the thermal reaction Δ_1); (b) the difference spectrum due to Δ_4.

The quantum yields of the $E,Z \rightarrow E,E$ and $E,Z \rightarrow Z,Z$ photoreactions can be calculated using the methods developed by Mauser [7]. One important assumption is that the quantum yields are independent of the excitation wavelength; this is a safe assumption for azobenzenophanes and also for azobenzenes in the region of one absorption band [12]. As we must consider two independent photoreactions ($s=2$), the development of the absorbance at two wavelengths λ_1 and λ_2 must be evaluated, and this leads to

$$\Delta A_{\lambda_1} = z_{10}\int F'\mathrm{d}t + z_{11}\int F'A_{\lambda_1}\mathrm{d}t + z_{12}\int F'A_{\lambda_2}\mathrm{d}t \quad (11)$$

$$\Delta A_{\lambda_2} = z_{20}\int F'\mathrm{d}t + z_{21}\int F'A_{\lambda_1}\mathrm{d}t + z_{22}\int F'A_{\lambda_2}\mathrm{d}t \quad (12)$$

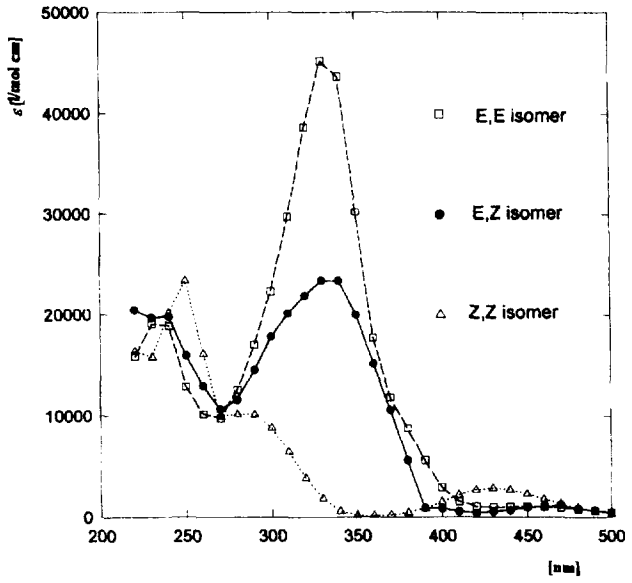

Fig. 7. Absorption spectra of the three main isomers of **2**.

where z_{ij} are constants containing absorption coefficients, quantum yields and initial absorbance values at the two wavelengths selected. Using all the reaction spectra, a matrix equation holds

$$\begin{pmatrix} \Delta A_{\lambda_1} \\ \cdot \\ \cdot \\ \cdot \end{pmatrix} = \begin{pmatrix} \Delta t & \int F' A_{\lambda_1} \mathrm{d}t & \int F' A_{\lambda_2} \mathrm{d}t \\ \cdot & \cdot & \cdot \\ \cdot & \cdot & \cdot \\ \cdot & \cdot & \cdot \end{pmatrix} * \begin{pmatrix} z_{10} \\ z_{11} \\ z_{12} \end{pmatrix} \quad (13)$$

$$\Delta A_{\lambda_1(m,1)} = A_{(m,3)} \cdot z_{\lambda_1(3,1)} \quad (14)$$

m is the number of reaction spectra included. On selection of a second evaluation wavelength, another matrix equation for ΔA_{λ_2} results. From the **Z** matrix, we can calculate the trace ($\mathbf{S} = z_{11} + z_{22}$) and determinant ($\mathbf{D} = [z_{11}z_{22}) - [z_{12}z_{21}]$)

$$\mathbf{S} = -(\varphi_{E,E \to E,Z}\varepsilon'_{E,E} + [\varphi_{E,Z \to Z,Z} + \varphi_{E,Z \to E,E}]\varepsilon'_{E,Z} + \varphi_{Z,Z \to E,Z}\varepsilon'_{Z,Z}) \quad (15)$$

$$\mathbf{D} = \varphi_{E,E \to E,Z}\varphi_{E,Z \to Z,Z}\varepsilon'_{E,E}\varepsilon'_{E,Z} + \varphi_{E,Z \to E,E}\varphi_{Z,Z \to E,Z}\varepsilon'_{Z,Z}\varepsilon'_{E,Z} + \varphi_{E,E \to E,Z}\varphi_{Z,Z \to E,Z}\varepsilon'_{E,E}\varepsilon'_{Z,Z} \quad (16)$$

All the absorption coefficients and quantum yields $\varphi_{E,E \to E,Z}$ and $\varphi_{Z,Z \to E,Z}$ are known; the two quantum yields $\varphi_{E,Z \to Z,Z}$ and $\varphi_{E,Z \to E,E}$ can be determined. The result is

$$\varphi_{E,Z \to E,E} = 0.23 \pm 0.07 \quad (17)$$

and

$$\varphi_{E,Z \to Z,Z} = 0.33 \pm 0.10 \quad (18)$$

3.4. Investigations of the thermal and photoreactions of 3

We have only a very limited amount of pure material of azobenzenophane **3**. Therefore only certain characteristic experiments have been performed. The main characteristics of photoisomerization are the same as those of **2**. The thermal stability of *Z,Z*-**3** matches that of *Z,Z*-**2** at least. However, we did not detect the very fast thermal reactions Δ_3 and Δ_4 after interruption of the irradiation of **3**.

4. Discussion

4.1. Spectra

The spectra of the *E,E*-azobenzenophanes are essentially *E-p,p'*-dimethylazobenzene spectra characterized by the low-intensity (symmetry forbidden) $n \to \pi^*$ band in the 400–500 nm region and the very intense (symmetry allowed) $\pi \to \pi^*$ band at 332 nm. However, there is an additional band of moderate intensity in the 380 nm region which appears in all azobenzenophanes. This may be due to the interactions of the transition moments as described by exciton theory [13]. When one or both azobenzene units are in the *Z* configuration, this band is missing. The *Z* isomer has different transition moments from the *E* isomer: the long-wavelength band is allowed, but the UV band is weak compared with that of the *E* isomer. The disappearance of the "cyclophane" band may be due to the low oscillator strength of the *Z* unit, reorientation of the transition moments in the *Z* unit compared with the *E* unit or rearrangement of the molecule removing the contact of the azobenzenes in the sandwich structure of the phane.

4.2. The influence of C_3 bridges

A most striking feature of the azobenzenes **2** and **3** is their thermal stability in the *Z,Z* form ($t_{1/2}$ = 400 days) [14] compared with **1** ($t_{1/2}$ = 5 days), azobenzene ($t_{1/2}$ = 2.5 days) and the pull-push substituted azobenzenes such as 4-dimethylamino-4'-nitroazobenzene ($t_{1/2}$ in the millisecond range). This seems to be due to the difference in flexibility of the $-CH_2-S-CH_2-$ and $-CH_2-CR_2-CH_2-$ bridges of the phanes.

Thus azobenzenes with a three-carbon bridge are bistable photoswitchable systems. They meet the requirements of a reversible optical storage element [15]. At a writing wavelength of 366 nm, the phane system is shifted to the *Z,Z* side, and at a writing wavelength of 436 nm, the phane system is shifted to the *E,E* side. Reading at 366 nm is virtually non-destructive as the *Z,Z* form has an extremely low absorption coefficient (as low as 180 l mol^{-1} cm^{-1}) and the *E,E* form, which absorbs about 70 times more strongly, is converted only into the *E,Z* form which quickly re-isomerizes to the *E,E* form. Thus the concentration of the strongly absorbing molecular form is re-established. Of course, the use of other features for reading instead of absorption, such as the refrac-

tive index, change in surface charge, etc., in suitably shaped devices [12] will permit totally non-destructive reading.

4.3. The formation of a tetrazetidine structure

The azobenzenophanes **2** and **3** show one feature which is needed to tackle the tetrazetidine problem, i.e. solubility. However, in the light of this work, it seems that the formation of the four-membered nitrogen ring on this pathway requires a rather flexible molecule which allows an easy approach of the two azo groups. Their distance in the phanes is not much more than the contact distance of aromatic systems (340 pm); 386 pm has been determined from the X-ray structure of **1** [16] and 384 pm has been calculated by a force field program [17]. The N–N distance in the tetrazetidine ring is about 140 pm, less than half of the original separation. It seems that the more flexible $-CH_2-S-CH_2-$ bridges can accommodate these changes better than the rigid $-CH_2-CH_2-CH_2-$ connections. More flexible structures of the phanes, e.g. by using bridges with four or five members, should favour the ultimate step of ring formation. However, the necessary preformation of the ring will no longer be provided by the molecular structure, but will become a matter of conformational fluctuations. This, in turn, will favour the isomerization reactions compared with the ring closure reaction. At present, we are considering flexible clamps containing a cyclohexane boat element. However, we call to attention the opposite philosophy of Prinzbach et al. [1], who tried to fix the nitrogen atoms of aliphatic azo groups in close proximity in very rigid structures so that only small changes in the positions of the atoms were necessary to form the ring.

From an analysis of the fragmentation in the mass spectra of **2** and the open structure **7**, we find a characteristic difference: for **2**, the two fragments $m/e = 365$ au and $m/e = 240$ au are detected, whereas in the mass spectrum of **7** these peaks are absent. This is indicative of the two *Z*-monoazobenzene-*p*-cyclophanes **8** ($m/e = 365$) and **9** ($m/e = 240$) with $-CH^+-C(COOEt)_2-CH_2-$ and $-CH_2-S-CH_2-$ bridges respectively, which would have their origin in a metathetic reaction of the tetrazetidine ring. Indeed, it was shown in a tandem mass spectrometer that the fragment of 365 au is a direct product of a species with a mass of 606 au. These *Z*-azobenzene-*p*-cyclophanes are certainly very short lived; Funke and Grützmacher [18] have been unable to synthesize them. Thus we have another indication of the tetrazetidine, but as yet no proof of its existence.

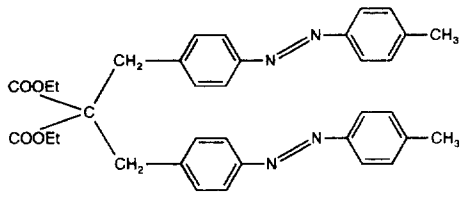

7

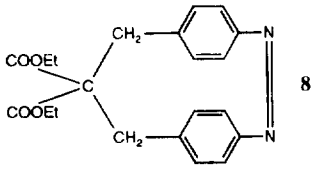

8

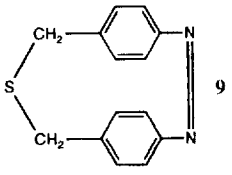

9

4.4. The fast thermal reactions Δ_3 and Δ_4

The fast thermal reactions Δ_3 and Δ_4 are not important in the whole isomerization system. However, they are puzzling in that a thermal isomerization from an *E* to a *Z* configuration takes place after 436 nm irradiation (which shifts the overall composition to the *E* side). The appearance of the phane band in the difference spectrum indicates that it is the *E,E* isomer that is formed (Δ_3) or disappears (Δ_4), and therefore the isomerization reactions of the *E,E* and *E,Z* isomers are involved. In simple azobenzene, the *Z* isomer is about 45 kJ mol^{-1} less stable than the *E* isomer, and therefore only $Z \rightarrow E$ isomerization is observed as a thermal reaction. In **2**, there seems to exist a driving force for a thermal $E,E \rightarrow E,Z$ isomerization, i.e. there is an *E,Z* isomer in a conformation of lower energy than the *E,E* isomer. This driving force could be provided by the steric strain of an unusual isomer or conformer of the *E,E* isomer. It should be noted that no material is lost in the photochemical reaction system of **2** on repeated 366/436 nm irradiation cycles.

This concept prompted us to expand our computational efforts. We used the force field program PCMODEL [17] (with a modified MM2 force field according to Allinger [19]) and included a restricted Hartree–Fock (RHF) calculation [20]. With these calculations, we realized that with widely different starting geometries two different minima are found for each of the isomers, one belonging to a sandwich form of the molecule and one to an open relatively flat form (*Z,Z*) or basket-like form (*E,Z*).

According to these calculations, the sandwich forms have MMX energies of 60.88, 300 and 315 kcal mol^{-1} and the open forms have energies of 187.3, 83.79 and 91.5 kcal mol^{-1} for the *E,E*, *E,Z* and *Z,Z* isomers respectively. We do not attribute importance to the absolute numbers, but to the qualitative picture. This indicates that the *E,Z* and *Z,Z* isomers are more stable in the open forms, and thus a large conformational change should occur on $E,E \rightarrow E,Z$ isomerization. However, experiments at 77 K in a rigid solvent indicate that isomerization is possible from the *Z,Z* to the *E,E* form in this solid matrix. Moreover, the resulting spectrum contains the cyclophane band, indicating a sandwich conformation. An open form to sandwich transformation is impossible in this matrix.

At present, the molecule isomerizing thermally from *E* to *Z* is unknown, and we can only speculate on its identity.

5. Conclusions

In this paper, we have reported the photochemistry of azobenzenophanes with two para bridges containing a C_3 chain. By exploiting the fact that interactions of the azobenzene units only appear in the spectrum of the *E,E* isomer in the cyclophane band near 380 nm, we determined the spectrum of the *E,Z* form which shows no such interactions, and with these coefficients we determined the quantum yields of all four photoisomerization steps.

The C_3 chain seems to provide more rigidity than structures with $-CH_2-S-CH_2-$ bridges. As a consequence, the *Z,Z* form is virtually thermally stable. This makes the azobenzenophanes with C_3 bridges potential candidates for optical data storage devices. On the other hand, the increased rigidity jeopardizes our intention to use azobenzenophanes as precursors for tetrazetidines. The necessary flexibility of the molecule to accommodate the contraction of the central part of the azo compounds on tetrazetidine formation seems to be lost.

Acknowledgements

We gratefully acknowledge the substantial support of the Deutsche Forschungsgemeinschaft and the help of Mrs. A. Woll in the syntheses. We thank Mrs I. Klaiber for measurement of the mass spectra and assistance in interpretation.

References

[1] H. Prinzbach, G. Fischer, G. Rihs, G. Sedelmeier, E. Heilbronner and Z.-Z. Yang, *Tetrahedron Lett., 23* (1982) 1251–1254.
[2] G. Ritter, G. Häfelinger, E. Lüddecke and H. Rau, *J. Am. Chem. Soc., 111* (1989) 4627–4635.
[3] H. Rau and E. Lüddecke, *J. Am. Chem. Soc., 104* (1982) 1616–1620.
[4] D. Röttger, *Ph.D. Thesis*, Hohenheim, 1995.
[5] N. Tamaoki, K. Ogata, K. Koseki and T. Yamaoka, *Tetrahedron, 46* (1990) 5931–5942.
[6] G. Gauglitz and G. Kraus, MESSEN VERSION 3.5©, Universität Tübingen, 1991.
[7] H. Mauser, *Formale Kinetik*, Bertelsmann Universitätsverlag, Düsseldorf, 1974. H. Mauser, *Z. Naturforsch. Teil B, 23* (1968) 1025–1033 (in short form, G. Ritter, G. Häfelinger, E. Lüddecke and H. Rau, *J. Am. Chem. Soc., 111* (1989) 4627–4635 Appendix).
[8] H. Mauser, *Formale Kinetik*, Bertelsmann Universitätsverlag, Düsseldorf, 1974, p. 212.
[9] R.M. Wallace and S.M. Katz, *J. Phys. Chem., 68* (1964) 3890–3892.
[10] D. Röttger, Ph.D. Thesis, Sect. 8.9.
[11] H. Lachmann, H. Mauser, F. Schneider and H. Wenck, *Z. Naturforsch. Teil B, 26* (1971) 629–638.
[12] H. Rau, Photoisomerization of azobenzenes, in J.F. Rabek (ed.), *Photochemistry and Photophysics*, Vol. II, CRC Press, Boca Raton, 1990, p. 125.
[13] A.S. Davidov, *Theory of Molecular Excitons*, McGraw-Hill, New York, 1962.
[14] H. Rau and D. Röttger, *Mol. Cryst. Liq. Cryst., 246* (1994) 143–146.
[15] H. Rau and D. Röttger, *German Patent 43 24 309*, 1994.
[16] G. Sawitzki and H. Rau, *Liebigs Ann. Chem.*, (1981) 993–998.
[17] C. Still, PCMODEL (VERISON 2.0), Serena Software, 1990.
[18] U. Funke and H.-F- Grützmacher, *Chem. Ber., 122* (1989) 1503–1508.
[19] N.J. Allinger, *J. Am. Chem. Soc., 99* (1977) 8127–8134.
[20] P.W. Atkins, *Quanta*, Oxford University Press, 1991, p. 327.